2. ORA OCCULTATION RADIOMETER ON EURECAINSTRUMENT DESCRIPTION AND PRELIMINARY RESULTS

Etienne Arijs,
Dennis Nevejans, Didier Fussen,
Piet Frederick, Emiel Van Ransbeeck

Belgisch Instituut voor Ruimte Aeronomie
Ringlaan 3, B-1180 Brussel
F.W. Taylor, S.B. Calcutt, S.T. Werret, C.L. Hepplewhite, T.M. Pritchard, I. Burchell.
Oxford University

ABSTRACT

A short description is given of the Occultation Radiometer which has been flown recently on the EURECA carrier. A brief outline of the scientific rationale, instrument characteristics and status of the data reduction is presented.

INTRODUCTION

Ozone is one of the most crucial components of our atmosphere. This gas, although only a minor constituent, is of vital importance since it prevents harmful solar UV radiation from penetrating to the Earth's surface. Decreasing its concentration may have dramatic effects on man's health and our ecosystem in general. The ozone layer is controlled by a complex mechanism, which is an interplay of dynamic and chemical phenomena in the atmosphere. Since the discovery of the Antarctic ozone hole [1, 2, 3], belief that man-made pollutants may have drastic effects on the ozone content increased considerably and research efforts within this field were intensified significantly. It became clear that, apart from natural and man-made chemicals such as the nitrogen oxides and chlorine compounds, aerosols play an important role in ozone chemistry [4, 5].
Any opportunity to measure ozone and related components on a long time scale and with global coverage should therefore be exploited. The EURECA carrier, proposed by ESA in the early eighties and mainly intended for microgravity research, offered an occasion to perform such measurements in a simple and relatively inexpensive way for at least 6 months with a longitudinal coverage, ranging from roughly 35°S to 35°N.
Therefore the Belgian Institute for Space Aeronomy (BISA) proposed for the EURECA mission a simple radiometer ORA (= *Occultation RAdiometer*) capable of measuring by means of an occultation technique in the visible and near UV part of the solar spectrum, ozone, NO_2, aerosols and water vapour. The proposal was combined with the one introduced by the Department for Atmospheric, Oceanic and Planetary Physics of the University of Oxford (UK) to measure upper atmospheric water vapour in the infrared. Although water vapour is very important for the chemistry and radiative balance of the atmosphere, measurements of its concentration in the upper atmosphere are still very limited [6]. The detailed balance of this component is determined by production (mainly through photolysis of methane at low-

er levels), transport from lower altitudes and escape to free space (in the form of atomic hydrogen, produced by photo dissociation of water itself). In order to understand this balance, again long term and global measurements are required. The combined proposal by BISA and the Oxford team was accepted by ESA and resulted in the instrument ORA, described hereafter.

EXPERIMENTAL

1 THE EURECA CARRIER AND THE MISSION

The EUropean REtrievable CArrier [7, 8] is the largest spacecraft ever built and flown by ESA. It weighed 4500 kg at launch and measured 20 m across. The payload of about 1 ton, 80 % devoted to microgravity research, consisted of 15 active experiments and 3 add-ons. Of these, 5 experiments were multi-user facilities developed under ESA contract and 10 were individual instruments built by European scientific institutes and industry.
EURECA provides about 1500 W of power, generated by solar panels, available to the different experiments. To optimize the performance of the solar panels, the spacecraft has a sunpointing capability with an accuracy of ±1°. EURECA was launched by the Space Shuttle "ATLANTIS" (STS46) from KSC on 31 July 1992 at 13:56 GMT. It was released from the Shuttle cargo bay on 2 August 1992 at an altitude of 424 km and subsequently maneuvered into its mission orbit, which was reached on 7 August 1992. The final orbit altitude was 508 km and the inclination 28.5°. The science operations started on 10 August 1992 and continued according to plan until the end of January 1993. On 26 January the freon cooling loop was deactivated, concluding the baseline science operations. Nevertheless some experiments, including the ORA instrument (see section 3), could remain active in the so-called dormant mode.
The orbital transfer maneuvers to bring EURECA to a lower orbit, where it could be captured again by the Space Shuttle started on 20 May 1993 and ended on June 8. On 21 June 1993 the shuttle "ENDEAVOUR" (STS57) was launched for the EURECA retrieval. Grappling of EURECA was performed on 24 June and on 1 July 1993 EURECA landed safely on Earth.

2 THE OCCULTATION TECHNIQUE

The sunpointing capabilities of the EURECA carrier make it a very suitable spacecraft to perform so-called solar occultation measurements, the geometry of which is shown in Figure 1. The approach of this method is to measure the attenuation of the solar radiation, due to absorption by atmospheric constituents, during sunrises or sunsets as seen by the satellite from its orbit around the Earth. During these occultations, the instrument measures through successive layers of the atmosphere, and as the satellite moves along its orbit the grazing height h changes (see fig 1). If the absorption properties of the atmospheric constituents are known, and measurements are performed at appropriate wavelengths, the concentration of the constituents in the different atmospheric layers can be derived from the observed signal as a function of grazing height. The retrieval of the concentration versus altitude profiles of atmospheric constituents requires a deconvolution procedure, which involves complicated mathematical techniques.
The major advantage of the occultation method, however, is that it is self calibrating. If the grazing height h (Fig. 1) is larger than the top of the atmosphere (generally about 100 km) the instrument measures a non attenuated signal. Since in the experiment, the absorption is determined by the ratio of the actual signal and the non attenuated signal, the calibration is actually performed in flight immediately before or after each occultation. Occultation by the solid Earth also provides an ideal zero-point calibration. Observation of sunset and sunrise from a satellite is only possible if the angle between the satellite orbit plane and the solar direction is within certain values. Due to the low orbital inclination this condition is always fulfilled for EURECA. The price for this is, however, a limited latitudinal coverage of the observations (in our case from roughly 35°S to 35°N).

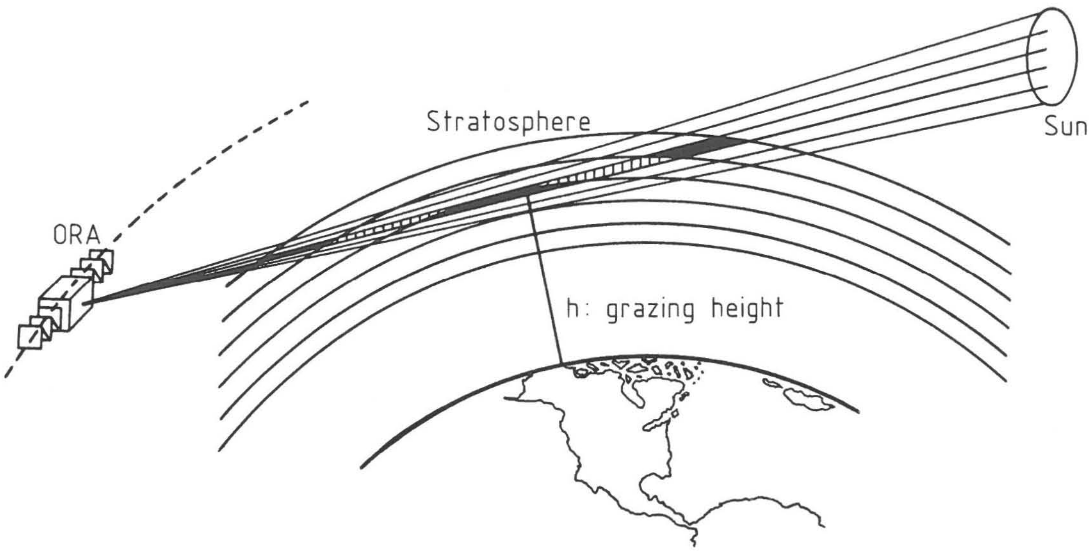

Figure 1 : Geometry of solar occultation experiment

3 THE ORA INSTRUMENT

3.1 Mechanical structure

The ORA instrument, schematically shown in Figure 2, has a total weight of 17 kg and consists of four major parts: the mechanical structure (A and B), the electronics unit (E), the UV-visible module (C) and the infrared unit(D). The Belgian Institute for Space Aeronomy has been responsible for the development of the mechanical structure, the electronics unit and the UV-visible unit. The infrared module was delivered by the Department for Atmospheric, Oceanic and Planetary Physics of the University of Oxford. The qualification of the flight model of the instrument, interfacing with ESA and management was provided for by BISA.
In view of the limited space on the EURECA carrier, the ORA instrument had to be mounted above another instrument (the Danish WATCH experiment) by means of a support structure (bridge). This bridge caused a number of mechanical problems with respect to vibration levels and required a careful mechanical design and simulation, the latter being performed by the Belgian company LMS (Leuven Measurement Systems). As a result of three prototypes and several vibration tests, a final model emerged, which is shown in Figure 2. To allow for the heat dissipation of the instrument, two heat pipes (F), constructed by SABCA, were integrated in the bridge.
EURECA being a carrier designed for microgravity, moving parts in the instrument had to be limited to a minimum. Therefore and in view of the weight and power budget, the ORA instrument has no sun tracking device. Instead, the field of view of the optical modules was chosen large enough (see section 3.2 and 3.3) to assure a full view of the Sun. As will be discussed further on, this has severe implications on the data reduction.

3.2 Electronics unit

The electronics unit (E in figure 2) was completely designed by BISA. A full description of it as well as of its associated software, also developed entirely at BISA, has been given elsewhere [9].
It consists of the following modules:
- a microprocessor board, running a real time multi-tasking programme controlling the experiment
- a command receiver board, to allow remote control via the Remote Acquisition Unit (RAU), connected

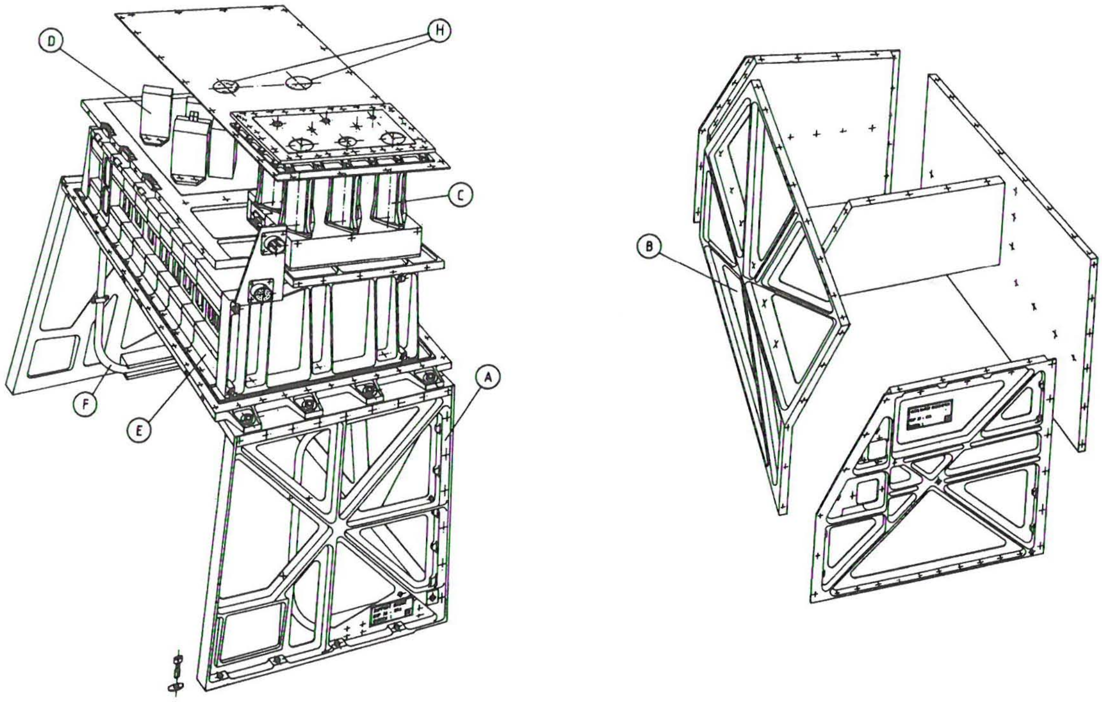

Figure 2: Overall view of the ORA instrument, showing the different subassemblies

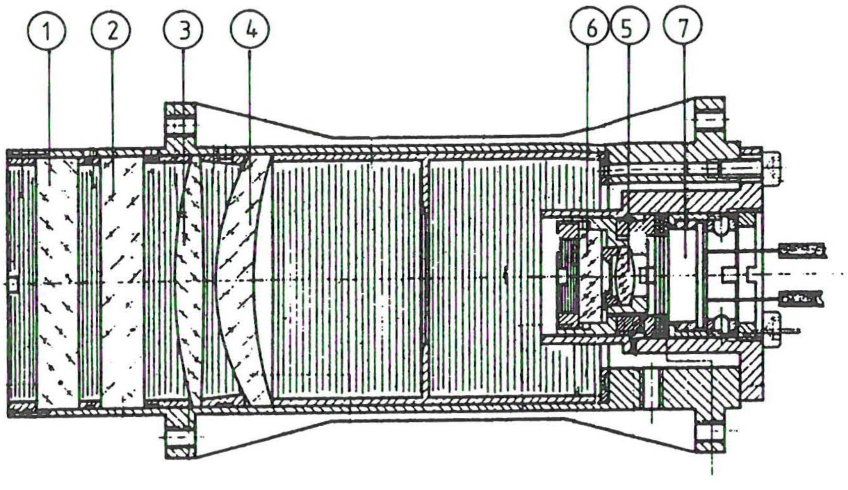

Figure 3: UV-visible module assembly. 1: quartz window; 2:interference filter; 3, 4 and 5 lenses; 6 : additional filter; 7:photodiode.

to the EURECA Data Handling System (DHS)
• a data transmitter board sending data formatted into telemetry or telecommand packets to a RAU connected to the DHS
• a synchronous detector board, containing 4 synchronous demodulators for the infrared module
• three integrated ADC boards each consisting of 4 programmable gain stages, 4 voltage to frequency converters and four 16bit counters.
• a housekeeping signal board, consisting of two multiplexers for 14 analog inputs and two ADC's.
• A motor and heater control for the Oxford infrared module.

The total power consumption of the complete ORA instrument is 25 Watt (at 28 Volt) if all heaters are operating.
After successful testing of the in house made prototypes, the space compatible flight electronics modules were constructed and qualified (vibration, thermal and EMC testing) by the Belgian company ETCA.

3.3 The UV-visible part

The UV-visible unit, designed to measure ozone, NO_2, water vapour and aerosols, through absorption measurements in the visible, near ultraviolet and near infrared part of the solar spectrum, consists of 8 similar modules, having the simple structure shown in figure 3.
Each module contains: a quartz window, an interference filter (IF) to isolate the appropriate wavelength domain, a simple optics to limit the field of view to ± 2° and a detector (either a Silicon photodiode or a GalliumPhosphide diode, depending on the wavelength).
The field of view of ±2° was chosen to guarantee a full view of the solar disc, taking into account the pointing accuracy of the EURECA carrier (± 1°) and possible misalignments of the ORA instrument with respect to the optical axis of the sun sensors of the spacecraft.
In some modules an additional small filter (a colored glass KG3 or an extra IF) is added just in front of the detector, to correct for some shortcomings in the main interference filter just behind the front quartz window. These additional correcting filters were introduced after the measurement of the transmission properties of the interference filters, manufactured according to our own specifications by the French company MATRA and prevented excessive transmission in the blocking bands of the main IF filters.
In front of the different modules, appropriate diaphragms were mounted to limit the light intensity, so as to enable operation in the linear domain of the photodiodes. The characteristics of the different UV-visible modules are summarized in Table 1.

Table 1: Characteristics of UV-visible modules

Main IF filter central wavelengh	Main IF filter band width	Main IF filter transmission	Photodiode Type	Correcting Filter
259 nm	23 nm	8.4 %	Si	> 270 nm
340 nm	6 nm	36 %	GaP	none
385 nm	3.4 nm	26 %	GaP	none
435 nm	3.2 nm	70 %	GaP	none
442 nm	3.3 nm	66 %	GaP	none
600 nm	9.5 nm	72 %	Si	KG3
943 nm	11 nm	74.5 %	Si	KG3
1013 nm	12.2 nm	54 %	SI	none

Although some IF filters were chosen to have their central wavelength in specific absorption bands of specific species (such as 259 nm in the Hartley bands for O_3, 600 nm in the Chapuis bands for O_3, 435 nm and 443 nm at a maximum and minimum of the NO_2 absorption and 943 nm in the absorption lines for water vapour), some overlapping absorption could not be avoided. Furthermore all modules are sensitive to absorption by aerosols and Rayleigh scattering. This additional difficulty, which complicates the data reduction, is unfortunately unavoidable.

3.4 The infrared part

The infrared part of the ORA instrument, known in the UK as *EOR*, is primarily designed for the measurement of water vapour in the upper atmosphere. Its location in the ORA instrument is shown in figure 2. The principle of operation and calibration of EOR was described in detail in the literature [10, 11] and its geometrical layout is shown in figure 4.

The instrument consists of two pairs of optical channels, which are identical except for the spectral response of the interference filter and the gas in the absorption cell. One pair of channels is used to measure water vapour, the other carbon dioxide. Assuming a homogeneous mixing of the latter gas up to about 100 km, the carbon dioxide data are merely used to determine total neutral densities.

Both pairs of channels being similar, we will only consider one here. The solar radiation, which enters the instrument through one of the entrance holes (H in figure 2) is reflected by a polished aluminum mirror inclined at 45° (A in figure 4). It then passes through an aperture stop and narrow interference filter (B), which selects the relevant spectral region and reaches a four blade rotating chopper (C). The latter modulates the beam at a frequency of 533.3 Hz and splits it in two portions. One beam passes through the chopper, bounces off another mirror (E) onto the lead sulphide detector (D0), whilst the other beam is reflected off the chopper blade, through a gas cell (G) onto another lead sulfide detector (D1).

The particular channel arrangement described above allows the atmospheric constituent to be measured in two ways. The simplest of the two methods, which is based upon the analysis of the signal of the detector seeing the light of the channel with no gas cell, is known as the "Wide Band" method. For this method preliminary results are available, which are described in section 3.3.3.

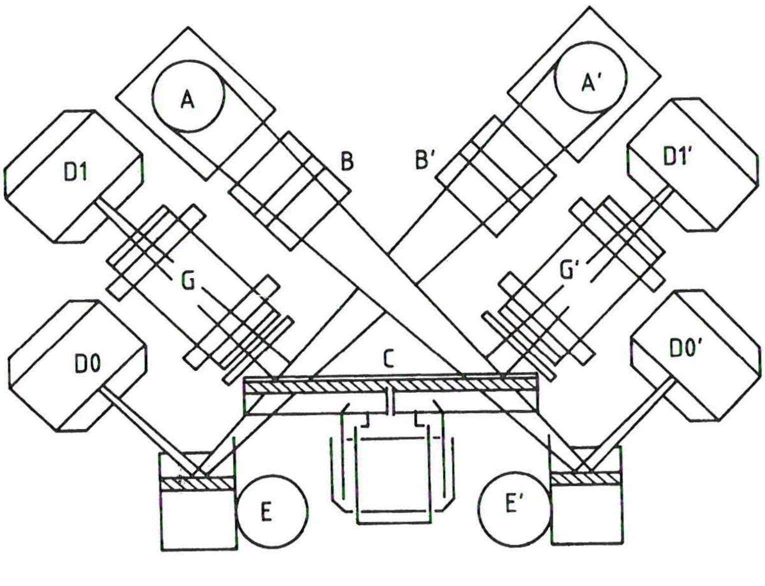

Figure 4: EOR instrument layout (for details see text)

The second method is a more complex, but more sensitive, differential technique, called the "Gas Correlation" method. It uses the signal of light modified by passing through the gas cell. One pair of channels has water vapour in the cell while, the pair looking at carbon dioxide has carbon dioxide in the cell. The purpose of the gas cell is as follows. Light that is only partially absorbed by the relevant atmospheric constituent will be nearly totally absorbed by the gas cell, which contains quantities of the gas to be analyzed. This means that no matter how much of the relevant constituent there is in the atmosphere, the detector signal will be the same. In other words, this detector will only be sensitive to all other absorbers in the atmosphere whilst the other (no cell) detector is sensitive to other absorbers and the relevant atmospheric constituent. The difference between these two calibrated detector signals is the signal due to the desired atmospheric constituent only.

Different criteria had to be taken into account for the choice of the interference filters for the EOR instrument. The low mass and power available to the ORA experiment, precluded the use of cooled detectors, restricting the experiment to short infrared wavelengths where there is sufficient solar signal (giving a better signal to noise ratio). The 2.7 micron region, where there is a vibration band of water available, appeared to be the most suitable. Another criterion was that the two spectral regions for water and carbon dioxide needed to be as close together in wavelength as possible, to make any scattering effect similar for both. Again 2.7 µm seems to be an ideal band, given the fact that CO_2 has spectral bands at 2.0 µm, 2.7 µm and 4.0 µm. The problem is however, that both CO_2 and H_2O bands overlap around 2.7 µm. As a compromise between overlap of species absorption, signal to noise ratio and filter availability, filters were chosen with a full width at half maximum of 70 cm^{-1} centred on 3900 cm^{-1} for water vapour and 3750 cm^{-1} for carbon dioxide.

The gas cells are 50 mm long and made of titanium. They have an internal diameter of 19 mm and are sealed by sapphire windows. Criteria considering Doppler shifting of the atmospheric lines by the line-of-sight component of the spacecraft velocity led to a partial pressure of 30 mb of water vapour (in a total pressure of 1 bar made up with nitrogen) for the water channel cell and a partial pressure of 320 mb CO_2 in a total pressure of 700 mb for the carbon dioxide channel. Heaters and thermistors are used to keep both cells at a temperature above 35°C during flight.

RESULTS AND DATA ANALYSIS

1 GENERAL

The ORA instrument was activated on 12 August 1992, and operated continuously for 10 months taking measurements at practically every sunset and sunrise. After a series of checkout activities (including temperature stabilization of the EOR gas cells) the first measurements started on 16 August 1992.

During the mission a continuous signal decrease occurred in two of the UV-vis channels (340 and 380 nm). This signal deterioration, however, was not dramatic in view of the high resolution of the ADC's and counters (16 bits) and the self calibrating properties of the instrument. The reason for the signal decrease is not clear yet, and has to be investigated after instrument recovery.

ORA was operated nominally (all UV-vis and infra red channels active) until deactivation of the EURECA freon loop (26 January 1993). Afterwards it was impossible to use the EOR part of the instrument, because, due to the high spacecraft temperature, the gas cell temperatures could not be stabilized anymore.

On 14 May, EURECA was commanded to Dormant Mode, i.e. with a pointing accuracy of ~5° and ORA operations were interrupted. Special measurements in full Sun were taken to characterize the instrument response to the pointing accuracy.

In total more than 6000 sunsets and sunrises were recorded. A typical example of the raw data as measured by ORA during a sunset is given in figure 5.

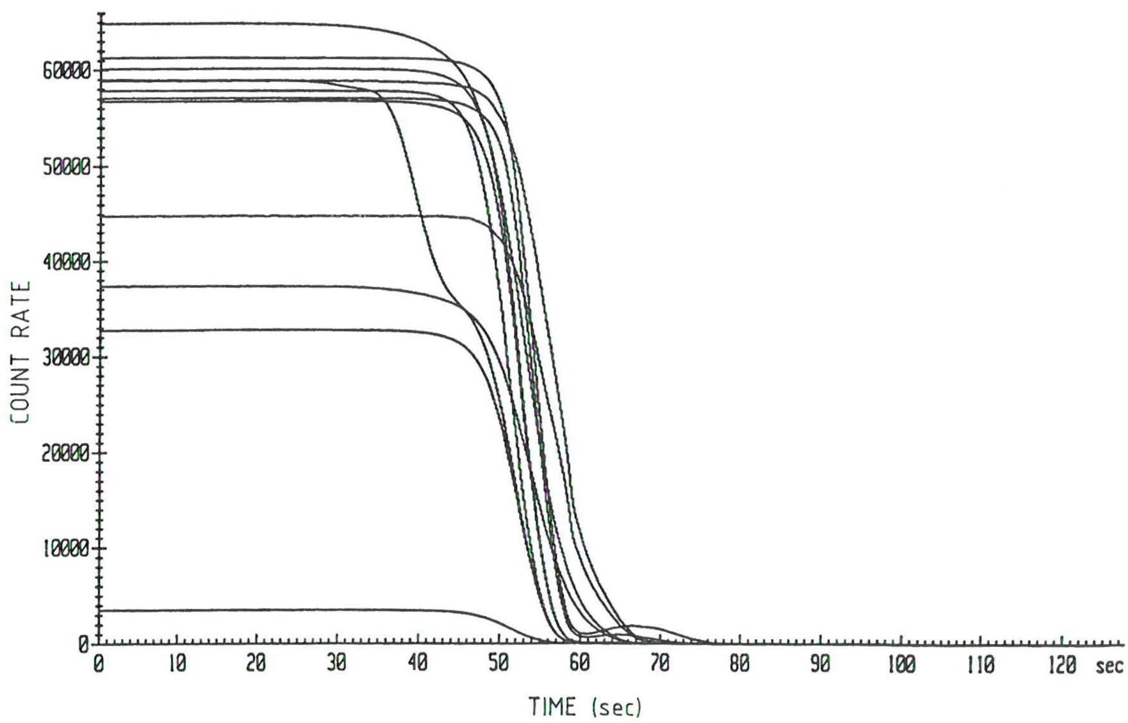

Figure 5: Raw data as transmitted by ORA, showing the decrease of light intensity as a function of time for the different channels

2 THE UV-VISIBLE DATA ANALYSIS

During each solar occultation, the UV-vis unit of the ORA instrument has continuously recorded the relative attenuation of the Sun's light in eight narrow wavelength domains (referred to hereafter as "channels"). This attenuation is caused by different mechanisms that can overlap in separate channels. The main processes involved are elastic scattering of light by small particles (including Rayleigh scattering by the atmospheric major constituents N_2 and O_2 and Mie scattering by aerosols consisting of dust and supramolecular clusters) and the photo absorption by trace gases such as ozone, NO_2 and water vapour. Elastic scattering of light gives rise to little wavelength dependency of the extinction coefficient while photo absorption total cross sections exhibit much more pronounced structures. The respective influences of these mechanisms can be summarized in table 2.

Table 2: Major light absorbers at the different UV-vis channels

λ [nm]	259	340	385	435	442	600	943	1013
predominant	O_3	neutrals	aerosol	aerosol	aerosol	O_3	aerosol	aerosol
constituents	neutrals	aerosol	NO_2	NO_2	NO_2	aerosol	H_2O	

The two channels 435 and 442 nm, chosen for NO_2 detection, are lying close together because the NO_2 photo absorption cross sections at those wavelengths, although not dominant, are quite different and well marked on the differential signal. Channels at 259 and 600 nm are more specific to ozone and 943 nm was selected for water vapour. The remaining channels are mainly devoted to the correlative measurement of elastic scattering processes at different wavelengths.
At any time during the occultation, the relative transmission of a solar ray, grazing the Earth at an altitude h can be written as:

$$T_\lambda(h) = \exp\left(-\int_{s1}^{s2} \beta_\lambda(h) ds(h)\right) \qquad (1)$$

where $\beta_\lambda(h)$ is the total attenuation coefficient along the optical path whose length element is described by the variable $s(h)$.For any of the channels:

$$\beta_\lambda(h) = \beta_\lambda^{Rayleigh} + \beta_\lambda^{Mie}(h) + \beta_\lambda^{O_3}(h) + \ldots \qquad (2)$$

The relative (with respect to the full Sun) signal measured by ORA reads:

$$S_\lambda(h) = \int_{\Delta\Omega} W(\Omega) T_\lambda(h(\Omega)) d\Omega \qquad (3)$$

because the instrument observes the whole solar disk within the solid angle $\Delta\Omega$ spanning more than 25 km along the grazing plane. The angular function $W(\Omega)$ expresses the relative light distribution across the Sun including area and solar limb darkening dependencies. Considering that

$$\beta_{ij} = \sigma_i n_j(h) \qquad (4)$$

for a particular absorber j where σ_i represents the cross section in the channel i, it is crucial to notice that the density profiles $n_j(h)$ we try to retrieve are obscured by three mathematical obstacles:
1. the measured signal results from a double integration leading to a loss of spatial resolution
2. the relation between $S_\lambda(h)$ and $n_j(h)$ is highly nonlinear and the uniqueness of the solution is often questionable
3. overlapping contributions between channels require a constrained retrieval algorithm.

The scheme to solve these problems and to get a good estimation of the $n_j(h)$ profiles is called the inversion algorithm. The structure of the retrieval procedure is governed by the flow chart of figure 6. This set of tasks can be divided into 7 groups, namely:
1. the flight data preprocessing
2. the optical segment generation
3. the total cross section compilation
4. the synthetic spectrum production
5. the development of the inversion algorithm itself
6. the data analysis automation
7. the error estimation, data validation and spatio-temporal interpretation.

The status of progress in those tasks is discussed in detail hereafter.

2.1 Flight data preprocessing

Throughout the flight a database was built up by regularly extracting scientific as well as technological housekeeping data from the EURECA Data Disposition system with a software developed at BISA. The scientific data represent a subset of this ORA database. A systematic extraction of the relevant data including the signal in the different channels as a function of universal time together with the measured position of the satellite expressed in an Earthfixed frame has been done. Combining these with routines giving the astronomical ephemerides, enabled us to determine the geometrical grazing height of any ray hitting the satellite as well as the geographical spreading of the sites where the occultations were measured. These data are shown in figure 7. As can be seen a latitudinal coverage of roughly 35 °S to 35 °N was obtained.

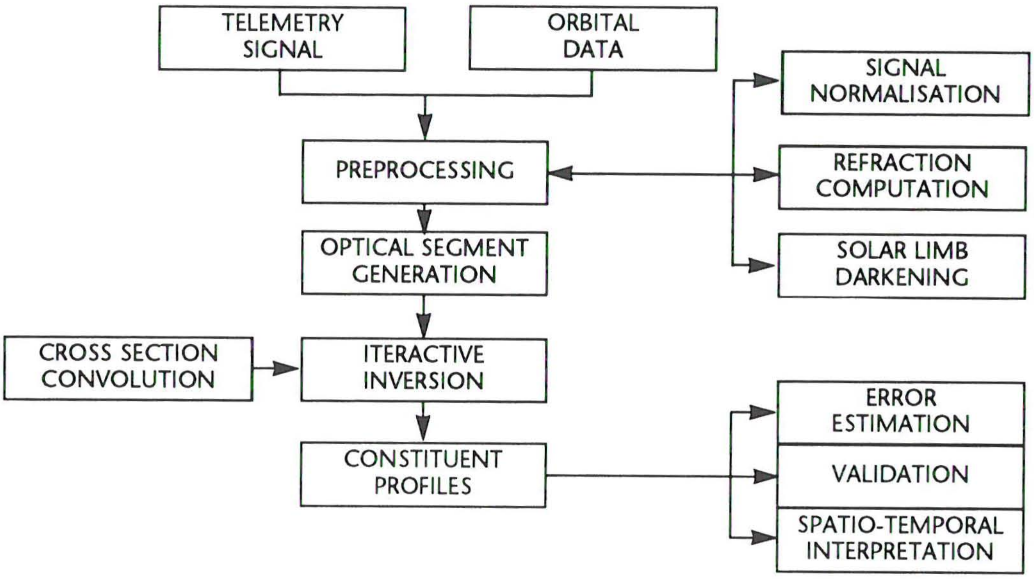

Fig. 6 Scheme for the retrieval procedure of the UV - vis data

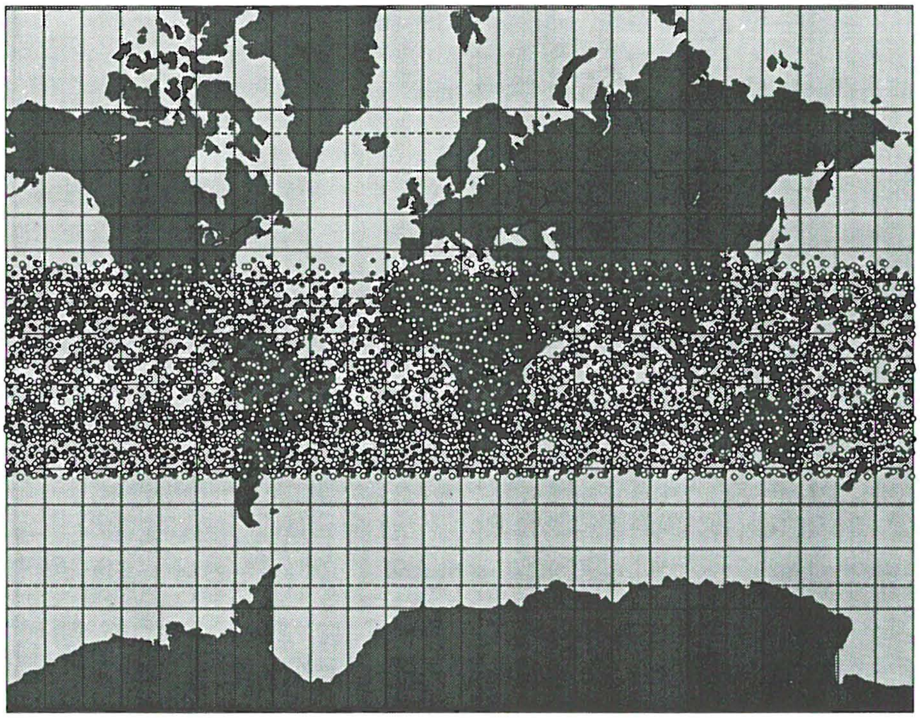

Figure 7: ORA observation sites

2.2 Optical segment generation

The atmosphere of the Earth is an inhomogeneous medium causing non-negligible refraction effects, especially below 35 km and for a large field-of-view instrument. In order to divide the atmosphere into a set of quasihomogeneous layers we wrote a complete code to solve this problem, taking into account the angular size of the Sun, solar limb darkening and the differential refraction attenuation. The results have been validated by comparison with similar calculations performed by other authors [12] and by inspecting the synchronization between the predicted occultation time and the observed one.

2.3 Total cross section compilation

The extinction coefficients have been computed for the directly exploitable channels including Rayleigh scattering, O_3, NO_2, H_2O and aerosol absorptions. A convolution of the best up-to-date absorption data with solar irradiance, detector wavelength sensitivity and transmission function has been performed. For water vapour absorption, the broadband model of Pierluissi [13] has been modified for weak absorptions and optimized with respect to the FASCODE package [14].

2.4 Synthetic signal production

For the retrieval scheme validation, we generated synthetic signals using the US Standard Atmosphere 1976 [15] and the low aerosol level compiled for the SAGE experiment data during the years 1986-1990 [16]. Comparison with ORA signal (fig 8) shows:

- a general good agreement validating astronomical, optical and extinction coefficient computations .
- the signature of an important supplementary absorption (probably due to aerosols from the Pinatubo eruption)
- the low apparent spatial resolution compensated by a high instrument sensitivity (NO_2 and H_2O signatures)

2.5 Development of the inversion algorithm itself

As appears from the mathematical expression of the signal, the occultation method leads to a nonlinear inversion problem. The first difficulty lies in the choice of an inversion method of high performance for the extinction coefficient profile (there are about "6000 events x 8 channels" to retrieve) which is at the same time robust, i.e. quite insensitive to the profile analytical properties.
This method has to face with the inherent degeneracy of the problem which can only be solved by an adequate regularization criterion. More subtle is the question of the maximal information content that we can extract from a given signal to get the maximal spatial resolution with a low retrieval error.
At the present time both above-mentioned points are under investigation.
From the obtained extinction profiles another inversion problem (fortunately linear) must then be solved to capture the relevant contributions embedded in an extinction profile. This is of course a constrained problem due to the correlative effects of one constituent amongst several channels.

2.6 Data analysis automation

When the whole retrieval algorithm is ready as a framework of independent optimized modules, it will then be necessary to define the best strategy for the data analysis concerning the possible necessity to work on averaged (latitude, longitude and time). Large storage capacities will be required and the use of a powerful graphical interface is desirable.

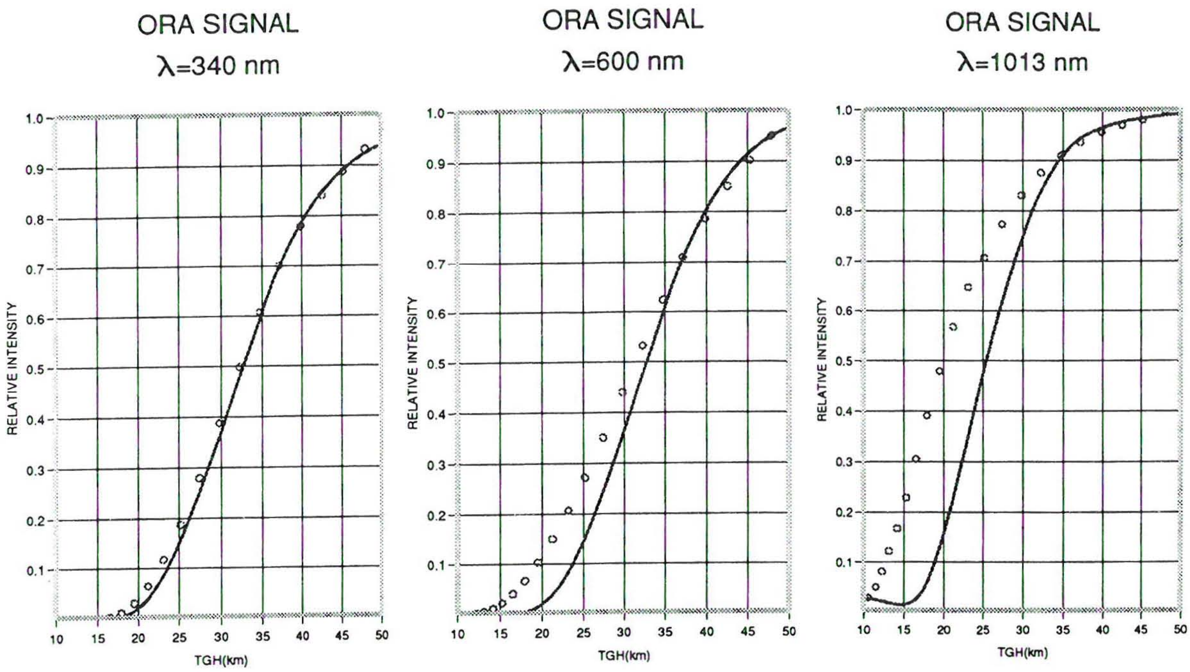

Figure 8: Comparison of calculated (synthetic) signal (open dots) with observed normalized signal at different wavelengths

2.7 Error estimation, validation and interpretation

A forward-backward error prediction scheme has to be developed to estimate the retrieval error as a function of constituent and altitude. This step will be a prerequisite for the validations of the ORA results with other space or groundbased experiments. Cooperative programmes and data exchange with other scientific teams will be highly profitable.
Last but not least, the retrieved density profiles $n_j(h)$ must be interpreted and compared with other results such as global 3D models, optical properties of aerosols and other studies.

3 THE INFRARED DATA

There are very few measurements of mesospheric water vapour, and as a result, very little is known about the chemistry and transport processes that occur. As previously explained, EOR measures mesospheric water vapour using four channels. So far, only the data from the two wide band channels have been investigated. One channel looks in a wavelength region centred at 3900cm^{-1} where water vapour is the only major absorber, and the other centered at 3750cm^{-1} where carbon dioxide and water vapour are the only major absorbers. If the amount of atmospheric carbon dioxide is assumed to be thoroughly mixed and known, the data from the carbon dioxide channel can be used to calculate the air density, from which it is possible to deduce pressure and temperature, assuming hydrostatic equilibrium.

3.1 The Forward Model

In order to retrieve the water vapour profile it is necessary to construct a forward model, wich calculates, for a given atmosphere what EOR will detect in the two channels.

The atmosphere is represented by a state vector consisting of air density and water vapour mixing ratio on a height grid from 32 to 108 km in 2 km intervals. An ideal forward model would then take this state vector and for each level, ray-trace a path through the atmosphere. The transmission would be calculated line by line over the non-homogeneous path and then integrated over the filter function and field of view. For this line by line calculation an existing programme package, GENLN2 [17] is available. Unfortunately this programme is very CPU intensive, taking several days of CPU time to calculate just one sunset. When one considers that in a typical retrieval the forward model has to be performed eighty times one realizes that some compromises must be made, the major ones being :

1) The Curtis-Godson approximation:

This method involves representing a non-homogeneous ray path by an homogeneous path with mass weighted temperature and pressures. A look-up table of the errors made in making this approximation was made to improve the accuracy of the forward model and it was found that these errors are not significant.

2) The use of look-up transmission tables;

Using the line-by-line programme GENLN2 to calculate the transmissions for these Curtis-Godson paths is still time consuming. Instead transmission look-up tables were constructed using GENLN2 for a variety of temperature, pressure and absorber amounts. A cubic spline interpolation is then performed when transmissions are looked up.

3) Non-monochromatic multiplication of transmission.

For the channel where absorption is due to carbon dioxide and water vapour, a multiplication of transmissions needs to be performed. This should be done monochromatically. However, since the transmissions looked up in the tables have been integrated over the filter function, this cannot be done. A look-up table of the error made by multiplying transmissions non-monochromatically was made to improve the accuracy and it was found that these errors are not significant.

The forward model works as follows. First it takes the atmospheric state vector and ray traces paths through the atmosphere, calculating the mass of carbon dioxide, water vapour and the Curtis-Godson average temperature and pressure for each path. Subsequently transmissions for carbon dioxide and water vapour are looked up in the transmission tables for each path and the transmissions for the two channels calculated. The transmissions are then integrated over the field of view (the entire shape of the sun) and mapped onto the same grid as the real measurements.

3.2 The Inversion

The inversion problem is as follows. A measurement **y** is made of the transmissions through the atmosphere from which the most likely state of the atmosphere **x** has to be determined, given that **x** and **y** are related by the matrix equation

$$\mathbf{y} = \mathbf{K}\mathbf{x} \qquad (5)$$

and that the covariance on the measurement of **y** and of the a priori state vector are given by the covariance matrix $\mathbf{S}_\epsilon$ and $\mathbf{S}_x$ respectively.

In the case of EOR the **K** matrix is not constant, but a function of **x**. This makes the problem nonlinear and means that a nonlinear retrieval scheme needs to be used. The particular scheme chosen was Newtonian Iteration [18].

The Newtonian Iteration method linearizes the forward model by expanding it as a Taylor series about a guessed value $\mathbf{x}_n$ of the solution,

$$\mathbf{Y}=\mathbf{Y}_n+\mathbf{K}_n(\mathbf{X}-\mathbf{X}_n)+O(\mathbf{X}-\mathbf{X}_n)^2 \qquad (6)$$

where $\mathbf{Y}_n$ is the value of **y** calculated at $\mathbf{x}_n$, and $\mathbf{K}_n$ is the partial derivative of the forward model with respect to **x** at $\mathbf{x}_n$. Assuming that the problem is not too nonlinear, the higher order terms can be ignored and Newtonian Iteration gives the iterative solution

$$\mathbf{x}_{n+1} = \mathbf{x}_0 + \mathbf{S}_x\mathbf{K}^T{}_n(\mathbf{K}_n\,\mathbf{S}_x\,\mathbf{K}^T{}_n + \mathbf{S}_\epsilon)^{-1}\,[\mathbf{y}-\mathbf{Y}_n-\mathbf{K}_n(\mathbf{x}_o-\mathbf{x}_n)] \qquad (7)$$

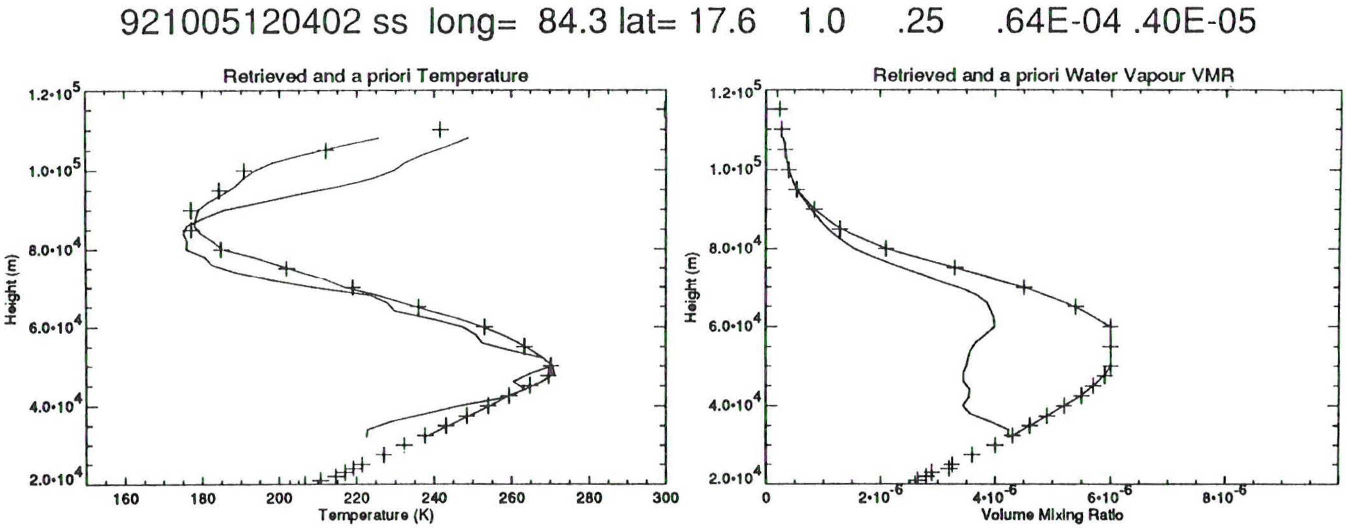

Figure 9: Typical retrieved temperature and water vapour mixing ratio profiles. (+++ A priori)

and the covariance of the solution is:

$$\hat{S} = (S^{-1}_{x} + \hat{K}^{T} S^{-1}_{\epsilon} K)^{-1} \qquad (8)$$

where $\hat{K}$ is K calculated at $\hat{x}$.

3.3 Results

We have studied the effect of altering various parameters in the retrieval scheme. Some of the effects investigated were:

1. Effect of K matrix recalculation ;
2. Effect of number of height levels in state vector ;
3. Effect of changing a priori climatology ;
4. Effect of changing covariance matrices ;
5. Effect of EURECA pointing instability.

Once some initial satisfactory values for the parameters were determined some retrievals could be performed. Figure 9 shows a typical retrieved temperature and water vapour profile on the same diagram as the a priori climatology used in the retrieval.

Once the code had been made to run quicker, retrievals were performed on all of the sunset data (the error on the sunrise data is much larger due to heating effects) up until the end of December. There are a few gaps in the data corresponding to periods when there were problems with the operation of EOR.

Figure 10 shows the retrieved zonal mean temperature and water vapour as a function of height between 02/11/92 and 30/11/92.

Even in these preliminary data, some structure is revealed that seems to be consistent from month to month. The retrieved numerical values for the air density and water vapour mixing ratio always seem to be lower than predicted by climatology. This probably indicates some sort of systematic error. One possible explanation could be an error in the tangent heights. Very recently, a height offset has been included into the state vector, and allowed to be retrieved. A typical retrieved value for this offset is about 0.5 km, which seems to be enough to make the retrieved profiles more acceptable (i.e. no longer always lower than the a priori climatology). This effect still has to be more closely investigated but initial results seem promising

Close analysis of the retrieval code for the wide band channels reveals that it should be possible to retrieve water vapour up to nearly 80 km, and temperature up to about 95 km.

3.4 Future Work

At the moment, retrievals are being performed using only the data from the wide band channels. Before attention can be paid to the gas correlation technique the retrieval code has to be further checked. The following still has to be done:
1.Perform some bulk retrievals including the height offset as a retrieved quantity.
2. Compare the retrieved profiles with the results of instruments that happened to be operating over the same geographical area and at the same time. This may be difficult as most instruments do not retrieve to as high an altitude as EOR. A good instrument to make a comparison with is the Halogen Occultation Experiment (HALOE) [19]. This instrument, on board UARS, has measurements taken at the same time as EOR and is also an occultation device.
3. Perform a full error analysis upon the whole retrieval scheme.
There are several things that need to be looked into. For instance, one effect to be examined is that due to other atmospheric constituents. There may be significant amounts of other gases that absorb in the same spectral region as the filters. The aerosol band at 30 km will also affect the retrievals. It may be possible to allow for this by using aerosol profiles retrieved by ORA.
Also, the current forward model assumes the sun to be at uniform temperature. The effect of a sun temperature distribution and of a solar spectra, though probably insignificant, needs to be investigated.
The gas correlation technique is more sensitive and may produce more interesting results, but the retrieval of them is more difficult. Several atmospheric transmission tables will be needed, each table differing by being convolved with a shifted gas cell transmission profile to take account of the Doppler shift.
Once the gas correlation retrieval code has been validated and an error analysis performed, an analysis can take place upon the retrieved water vapour spatial and temporal distribution. Hopefully some of the questions about mesospheric water vapour can be answered and a greater understanding will result.

CONCLUSIONS

During the 11 months that the EURECA mission lasted, the ORA instrument has been measuring almost continuously for about 9 months. Occultation data in the UV-visible were recorded successfully at each sunrise and sunset, apart from a few occasions where measurements were interrupted for short periods, due to operational requirements. The infra-red part of ORA (EOR) has collected data for more than 4 months. In total more than 6000 occultation events have been captured. As a result a huge volume of information concerning the composition of the Earth's atmosphere has been gathered, with a latitudinal coverage from 35°S to 35°N.
Although the conversion from the raw data into scientific results has not yet been fully completed, the preliminary results look very promising. It is hoped that the results of the infra-red experiment will contribute largely to our understanding of the mechanisms controlling the water vapour budget in the upper atmosphere. The retrieval of the UV-visible data is also expected to be most interesting and instructive, especially in view of the effects of the Pinatubo volcanic eruption on the ozone and aerosol concentrations. These concentrations should be mainly affected in the equatorial regions, where ORA has performed most of its measurements.

ACKNOWLEDGEMENTS

The authors are indebted to their respective governments for the financial support to make this experiment possible. The cooperation of the following companies has also been most appreciated: ETCA (Charleroi, Belgium), OIP (Oudenaarde, Belgium), LMS (Leuven, Belgium) and SABCA (Brussels, Belgium).

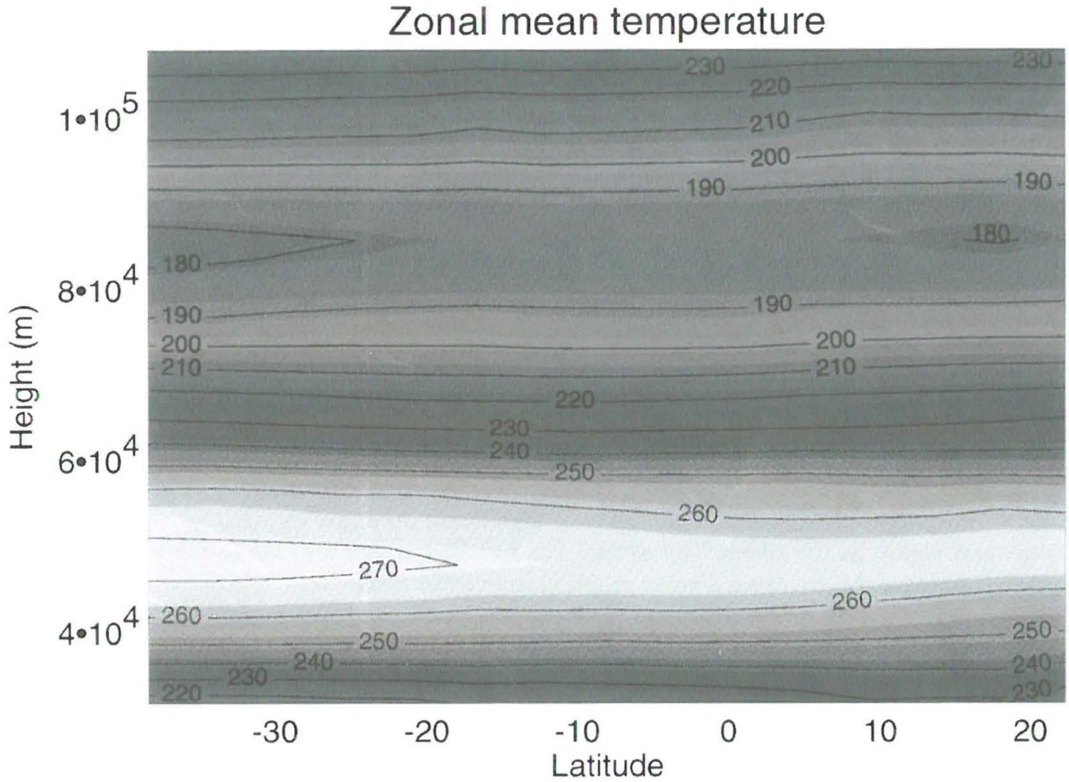

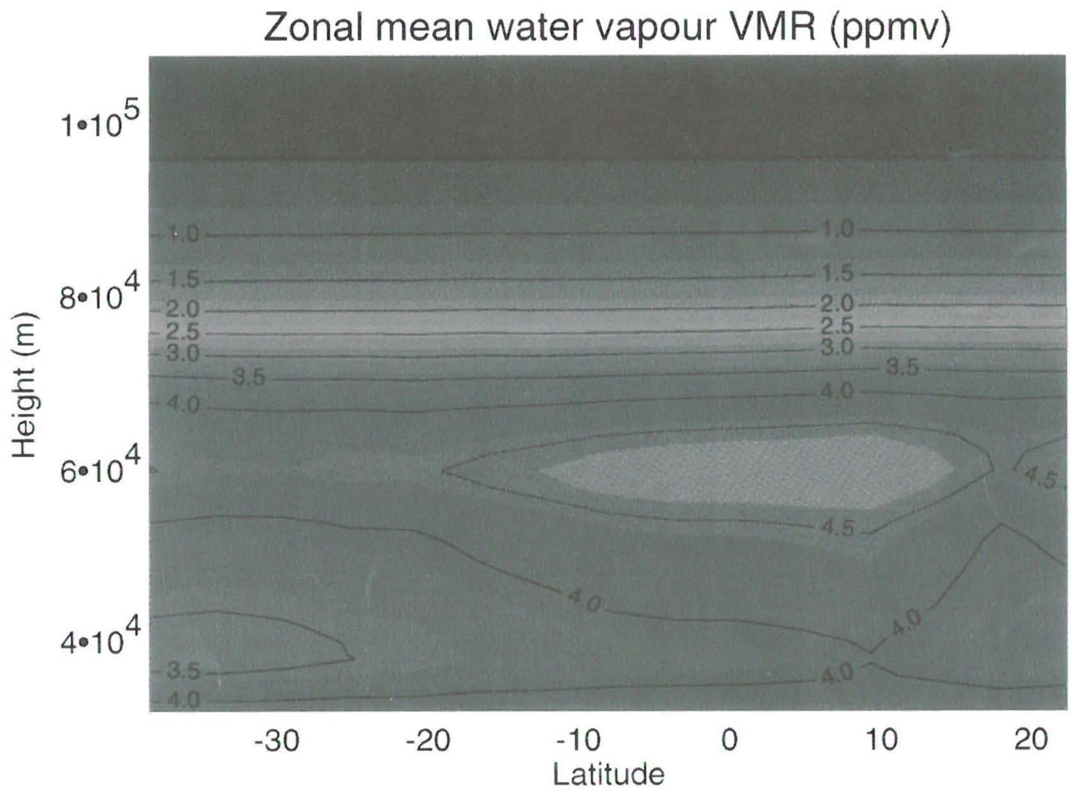

Figure 10 : First attempt showing retrieved zonally averaged temperature and water vapor mixing ratio between 02/11/92 and 30/11/92.
See also the colour version of fig 10 on page 169.

We would also like to express our gratitude and congratulations to the EURECA team of ESA-ESTEC and ESA-ESOC and to the technical staff of ESTEC for giving technical support during the development of the instrument and for making the EURECA mission a complete success.

REFERENCES

1. J. C. Farman, B. G. Gardiner, and J. D. Shanklin, "Large losses of total ozone in antarctica reveal seasonal ClO_x/NO_x interaction," *Nature*, vol. 315, pp. 207-210, 1985.

2. G. S. Henderson, G. C. McConnel, S. R. Beagley, and W. F. Evans, UPolar ozone depletion: current status," *Can. J. Phys.*, vol. 69, pp. 1110-1122, 1991.

3. S. Solomon, "The mystery of the antarctic ozone hole," *Rev. Geophys.*, vol. 26, pp. 131-148, 1988.

4. J. P. D. Abbat and M. J. Molina, "The heterogeneous reaction of HOCI + HCI $\mapsto C_{12} + H_2O$ on ice and nitric acid trihydrate: reaction probabilities and stratospheric implications," *Geophys. Res. Lett.*, vol. 19, pp. 461-464, 1992.

5. R. J. Salawitch, S. C. Wofsy, and M. B. McElroy, "Influence of polar stratospheric clouds on the depletion of antarctic ozone," *Geophys. Res. Lett.*, vol. 15, pp. 871-874, 1988.

6. S. Solomon, E. E. Ferguson, D. W. Fahey, and P. J. Crutzen, "On the chemistry of H_2O, H_2 and meteoritic ions in the mesosphere and lower thermosphere," *Planet. Space Sci.*, vol. 30, pp. 1117-1126, 1982.

7. W. Nellessen, "The EURECA project From concept to launch," *ESA Bulletin*, vol. 70, pp. 16-25, 1992.

8. L. Innocenti and D. Mesland, "Scientific utilisation of EURECA1," *ESA Bulletin*, vol. 70, pp. 26-35, 1992.

9. D. Nevejans, E. Arijs, and D. Fussen, "The electronic and software design of the ora occultation radiometer.," in *Proc. IVth Int. Seminar: Manufacturing of scientific space instrumentation*, (V. M. Balebanov, ed.), (Moscou), pp. 61-73, Academy of Sciences of the USSR, 1990.

10. S. B. Calcutt, T. M. Pritchard, C. L. Hepplewhite, F. W. Taylor, S. T. Werret, E. Arijs, and D. Nevejans, UA radiometer for the measurement of water vapour in the upper atmosphere from space,"*Applied Optics*, vol. 32, pp. 6764-6776, 1993.

11. T. M. Pritchard, *Sudies of minor constituents in the atmosphere*, PhD thesis, Oxford University, 1988.

12. I. Burchell, «Water vapour retrievals from EOR," Tech. Rep., Atmospheric, Oceanic and Planetary Physics, Dept. of Physics, University of Oxford, October 1993.

13. C. Pierluisi, C. Maragoudakis, and R. TheraniMohaved, "New LOWTRAN band model for water vapour," *Applied Optics*, vol. 28, pp. (3792-3795, 1989.

14. H. J. P. Smith, D. J. Deube, M. E. Gardner, S. Clough, F. X. Kneizys, and L. S. Rothman, FASCODE *Fast Atmospheric Signature Code (Spectral transitance and radiance)*,Visidyne, Inc., Burlington, MA, USA, 1978 (The version used here was PCnTRAN from Ontar Corp., Brooklyne, MA, USA).

15. U.S. *Standard Atmosphere, 1976*,National Oceanic and Atmospheric Organization, National Aeronautics and Space Administration, United States Air Force, Washington, DC, October 1976.

16. C. Brogniez and J. Lenoble, "Analysis of 5 year aerosol data from the Stratospheric and Gas Experiment,» *J. Geophys. Res.*, vol. 96, pp. 15,479-15,497, 1991.

17. D. Edwards, GENLN2: *A general line-by-line atmospheric transmittance and radiance model, version 3.0*, NCAR, Technical Note, NCAR/TN367+STR.

18. C. D. Rodgers, "Retrieval of atmospheric temperature and composition from remote measurements of thermal radiation.," *Rev. Geo. Space Phys.*, vol. 14, pp. 609-624, 1976.

19. J. M. Russel, L. L. Gordley, J. H. Park, S. R. Drayson, W. D. Hesketh, R. J. Cicerone, A. F. Tuck, J. E. Frederick, J. E. Haries, and P. J. Crutzen, "The HALOGEN occultation experiment.,» *J. Geophys. Res.*, vol. 98, pp. 10,777-10,797, 1993.